Materials Transactions, JIM, 48, pp.1412-1416, 2007.

Effects of grain-boundary sliding and plastic deformation of grains on the formation of grain-boundary cracks in a double cylindrical bicrystal of a Cu-SiO_2 alloy

Masakazu Seki[1,*1], Mitsuru Fujimoto[2,*1], Toshiyuki Fujii[1],

Masaharu Kato[2] and Susumu Onaka[2]

[1]*Department of Innovative and Engineered Materials*

[2]*Department of Materials Science and Engineering*

Tokyo Institute of Technology

4259-J2-63 Nagatsuta, Yokohama 226-8502, Japan

Abstract

A double cylindrical bicrystal is a bicrystal consisting of a cylindrical inside grain with a second grain wrapped around its curved side surface. Using a double cylindrical bicrystal of a Cu-SiO_2 alloy, tensile tests were performed at 800K under 2×10^{-4} / s . Three specimens cut from the same bicrystal were deformed to three different strains. Preferential formation of grain-boundary cracks around the cylindrical inside grain was observed after the tensile tests. In addition to the occurrence of grain-boundary sliding, the misfit of slip deformation at the grain boundary affects the formation of the grain-boundary cracks.

Keywords: grain boundaries; fracture; high temperature deformation; copper alloys----------

*1 Graduate student, Tokyo Institute of Technology

1. Introduction

At elevated temperatures, deformation or fracture behavior of polycrystals is affected by grain boundaries. To discuss the effects of grain boundaries, experiments using bicrystals have been performed in many previous studies, for example [1-4]. Bicrystals containing flat boundaries have frequently been adopted as simplified model materials for polycrystals. However, in the present study, we investigate the fracture behavior of a bicrystal that does not have a flat boundary.

A double cylindrical bicrystal is a bicrystal consisting of a cylindrical inside grain with a second grain wrapped around its curved side surface. Double cylindrical bicrystals have been used to discuss the inclination-angle dependence of the grain-boundary energy under fixed orientation relationships between grains [5,6]. In the present paper, we study the formation of grain-boundary cracks at elevated temperatures using a double cylindrical bicrystal of a Cu alloy containing small SiO_2 particles. The Cu-SiO_2 alloy was selected since brittle grain-boundary fractures are expected to occur in Cu alloys when they contain small grain-boundary particles [7,8]. Although deformation behavior at room temperature has been studied for a Cu double cylindrical bicrystal [9], fracture behavior of the bicrystal at elevated temperatures has not been studied.

Usual bicrystals containing flat boundaries lack one important characteristic of polycrystals that most of the grains are embedded in and surrounded by other grains. On the other hand, in a double cylindrical bicrystal, the cylindrical inside grain is surrounded by another outside grain. The characteristic of embedded grains is included in a double cylindrical bicrystal in a simplified manner. Considering this characteristic, we discuss the effects of grain-boundary sliding (GBS) and plastic deformation of grains on the formation of grain-boundary cracks.

2. Experimental

A double cylindrical bicrystal of a Cu-0.032mass%Si alloy was grown by the Bridgman method. The diameter of the whole bicrystal consisting of the inside grain (IS grain) and the outside grain (OS grain) was 40mm. The shape of the grain boundary between the IS and OS grains was determined by metallographic observation of the round slices cut from the bicrystal (Fig. 1(a) and (b)). The grain boundary between the IS and OS grains is a high-angle boundary. The orientation relationship between the two grains is not special, i.e., is not explained by the coincident site lattice model up to $\Sigma = 39$. As shown in Fig. 1(b), the trace of the grain boundary on the top surface of the slice has a shape close to a circle.

To obtain SiO_2 particles in the grains and on the grain boundary, the round slices of the bicrystal were internally oxidized with a Cu-Cu_2O-Al_2O_3 (weight ratio 1:1:2) mixed powder at 1223K for 72h. After the internal oxidation and the annealing under vacuum at 1223K for 72h, the average diameters of the SiO_2 particles in the bicrystal were about 0.8 μm for those on the grain boundary and about 0.3 μm for those in the grains.

Tensile specimens with a gage length of 22mm and a cross-sectional area of 20mm $\times$ 2mm were cut from the bicrystal. The shape of the bicrystal specimens is shown in Fig. 2(a). To describe orientations of the bicrystal in a consistent manner, the $x_1 - x_2 - x_3$ coordinate system shown in Fig. 2(a) is used, where the x_1-axis is the tensile axis and the x_3-axis the direction normal to the top surface of the bicrystal. Using this coordinate system, the orientations of the IS and OS grains are shown by a pair of stereographic projections in Fig. 2(b). Three tensile specimens having the same orientations were cut from the double cylindrical crystal. The IS grain has an orientation where plastic deformation by single slip is expected to occur. However, the tensile axis of the OS grain is almost parallel to [100] and multiple slip is expected

to occur from the early stage of plastic deformation. The angle θ measured from the stress axis shown in Fig. 2(a) will be used to indicate locations on the circular grain boundary.

After mechanical and electrolytic polishing, fiducial lines parallel to the x_1- and x_2- axes were scribed on the surface of one specimen at a spacing of $100\,\mu$m. The fiducial lines were used to measure the amount of GBS. The accuracy of the measurement depending on sharpness of the fiducial lines is about $1\sim2\,\mu$m. The tensile tests were performed in an argon-gas atmosphere with an Instron-type testing machine at 800K under an initial strain rate of 2×10^{-4}/s. The testing temperature of 800K was selected since significant intermediate temperature embrittlement is expected to occur for Cu polycrystalline alloys containing small oxide particles [7,8]. Deformation of the specimens was interrupted at certain strains and microstructural observations of the specimens were made after the tensile tests.

3. Results

3.1 Stress-strain curves

Figure 3 shows the nominal stress-plastic strain curves, the σ-ε curves, of the Cu-SiO_2 bicrystal at 800K under 2×10^{-4}/s. Tensile tests of specimens D1 and D2 were interrupted at $\varepsilon\approx0.02$ and 0.04, respectively. For specimen D3, the stress σ becomes a maximum $\sigma\approx25$MPa at $\varepsilon\approx0.08$ and after that σ decreases gradually with increasing ε. Breaking up of specimen D3 did not occur until $\varepsilon\approx0.18$, where the deformation of this specimen was interrupted. As will be shown later, such deformation behavior of specimen D3 comes from the formation of a large crack along the cylindrical grain boundary. Specimens D1 to D3 show similar stress-strain relationships for overlapping ranges of ε.

3.2 Microstructural observation

Occurrence of GBS was observed on the top surface of specimen D1 deformed until $\varepsilon \approx 0.02$. Figure 4 shows the variation in the amount d of GBS as a function of the angle θ defined in Fig. 2(a). As shown in Fig. 4, d becomes large around $\theta \approx \pi/4$, $3\pi/4$, $5\pi/4$ and $7\pi/4$. The driving force of GBS is the tangential traction acting on the grain-boundary plane. The peak angles $\theta \approx \pi/4$, $3\pi/4$, $5\pi/4$ and $7\pi/4$ are understood to be the orientations of the grain boundary where the driving force of GBS becomes large under the applied tensile stress. No grain-boundary crack was observed for specimen D1.

Grain-boundary cracks were observed on the top surface of specimen D2 deformed until $\varepsilon \approx 0.04$. Figures 5(a) to (d) are optical micrographs showing the surface of specimen D2. The inset in Fig. 5 shows the locations in specimen D2 from which Figs. 5(a) to (d) were taken. As shown in Figs. 5(a) and (d), grain-boundary cracks were clearly observed at the locations around $\theta \approx 3\pi/4$ and $7\pi/4$. These cracks extended for ranges of about $\pi/4$ on the top surface and penetrated the specimen along the thickness direction, i.e., the direction parallel to the x_3-axis in Fig. 2(a). The diagonal locations of the two grain-boundary cracks around $\theta \approx 3\pi/4$ and $7\pi/4$ correspond to the locations where large GBS was observed as shown in Fig. 4 for specimen D1. However, although similar large GBS occurred around $\theta \approx \pi/4$ and $5\pi/4$ for specimen D1, no cracks were observed at the same locations in specimen D2 as shown in Figs. 5(b) and (c). The preferential formation of grain-boundary cracks will be discussed in the Discussion.

Figure 6 is an optical micrograph showing a large grain-boundary crack in specimen D3 that was deformed until $\varepsilon \approx 0.18$. This large crack may be formed by the growth of the crack around $\theta \approx 7\pi/4$, which is shown in Fig. 5(d). Figures 5(a) and (d) show the importance of the tangential traction acting on the grain-boundary plane for the formation of grain-boundary cracks. On the other hand, Fig. 6 shows the

importance of the normal traction for the growth of grain-boundary cracks. Although the grain boundary in specimen D3 was seriously fractured, breaking up of the specimen did not occur because of the cylindrical shape of the grain boundary. This fracture behavior explains the gradual decrease of σ in the stress-strain curve of specimen D3.

4. Discussion

Grain-boundary cracks were formed in specimen D2 at the diagonal locations of about $\theta \approx 3\pi/4$ and $7\pi/4$, where large GBS was observed. This is understood since the occurrence of GBS is a major reason for intergranular brittle fracturing of polycrystalline materials, in particular, those which contain small grain-boundary particles [7,8]. However, formation of the grain-boundary cracks was preferential and no cracks were observed in the same specimen D2 at the other diagonal locations, about $\theta \approx \pi/4$ and $5\pi/4$, where similarly large GBS was observed. The large grain-boundary crack in specimen D3 shown in Fig. 6 also suggests that the grain-boundary around $\theta \approx \pi/4$ and $5\pi/4$ is infeasible for crack formation. As shown by slip lines observed in Figs. 5, plastic deformation during the tensile tests also occurred actively for both the IS and OS grains. Here we discuss the above preferential formation of grain-boundary cracks by considering the effect of misfit of plastic deformation at the grain boundary.

If the IS and OS grains are isolated, we can expect uniform deformation of the grains under the applied tensile stress. We evaluate the uniform deformation of the grains using the plastic distortions $\alpha_{ij} = \partial u_i / \partial x_j$ where u_i are the displacements. We consider the simple shear γ generated by operation of the primary slip system of the IS grain marked in Fig. 2(b). The simple shear γ causes the plastic distortions $\alpha^{\mathrm{I}}_{ij} = \partial u^{\mathrm{I}}_i / \partial x_j$ expressed by the $x_1 - x_2 - x_3$ coordinate system written as

$$\left(\alpha_{ij}^{\mathrm{I}}\right)=\gamma\begin{pmatrix}0.409 & 0.485 & 0.563\\ -0.054 & -0.065 & -0.075\\ -0.250 & -0.296 & -0.344\end{pmatrix}. \qquad (1)$$

On the other hand, the tensile axis of the OS grain is almost parallel to [100] and multiple slip is expected to occur. Slip lines due to the slip plane marked in Fig. 2(b) were mainly observed for the OS grain. When the multiple slip system of the OS grain marked in Fig. 2(b) operates as much as $\gamma/2$ for each slip direction, the plastic distortions $\alpha_{ij}^{\mathrm{O}}=\partial u_i^{\mathrm{O}}/\partial x_j$ expressed by the $x_1-x_2-x_3$ coordinate system are written as

$$\left(\alpha_{ij}^{\mathrm{O}}\right)=\gamma\begin{pmatrix}0.407 & 0.038 & 0.579\\ -0.035 & -0.003 & -0.050\\ -0.283 & -0.027 & -0.403\end{pmatrix}. \qquad (2)$$

The changes in the shapes of IS and OS grains by the uniform deformation are calculated from (1) and (2). Figures 7(a) and (b) show respectively the two-dimensional shape changes of the IS and OS grains on the x_1-x_2 plane, where the origin of the displacements are assumed to be located at the center of the circular grain boundary. However, since the IS and OS grains compose the double cylindrical bicrystal, the hypothetical uniform deformation may cause deficit or overlap of material at the grain boundary. This deficit or overlap of material is expressed by the difference in the displacements $\Delta\boldsymbol{u}=\boldsymbol{u}^{\mathrm{O}}-\boldsymbol{u}^{\mathrm{I}}$ at the grain boundary, where $\boldsymbol{u}^{\mathrm{I}}$ and $\boldsymbol{u}^{\mathrm{O}}$ are the displacements for the IS and OS grains, respectively.

The difference in the displacements $\Delta\boldsymbol{u}$ has a normal component Δu_{N} and a tangential component Δu_{T} with respect to the boundary plane. Although GBS can relax Δu_{T}, it cannot relax Δu_{N}. At elevated temperatures where GBS occurs, Δu_{N} is a measure of the misfit of slip deformation between IS and OS grains that affects the formation of grain-boundary cracks. That is to say, $\Delta u_{\mathrm{N}}>0$ means a deficit of

material at the grain boundary, which enhances the formation of grain-boundary cracks. The locations on the grain boundary where values of Δu_{N} are positive and large are feasible for the formation of cracks. On the other hand, locations where the values of Δu_{N} are negative are infeasible. In usual bicrystals containing flat boundaries, this effect of Δu_{N} vanishes since grain boundaries constrain only one side of the grains. The effect of Δu_{N} is important in polycrystals where most of the grains are embedded in and surrounded by other grains.

Figures 8(a) and (b) are, respectively, the variation of Δu_{N} shown by illustration of the double cylindrical bicrystal and the normalized variation of $\Delta u_{\mathrm{N}} / (\gamma r)$ as a function of θ, where r is the radius of the circular grain boundary. The results shown in Figs. 8 are calculated by using the distortions given by (1) and (2). Since Δu_{N} is the normal component on the circular grain boundary, calculations using the strains $\varepsilon_{ij} = \left(\partial u_i / \partial x_j + \partial u_j / \partial x_i\right) / 2$ in the IS and OS grains instead of the distortions $\alpha_{ij} = \partial u_i / \partial x_j$ give the same θ dependence of Δu_{N} as those shown in Figs. 8. The regions I and II around $\theta \approx 3\pi / 4$ and $7\pi / 4$ in Figs. 8 are the regions where GBS becomes large and, moreover, Δu_{N} reaches a maximum. This is in agreement with the preferential crack formation at around $\theta \approx 3\pi / 4$ and $7\pi / 4$. Although large GBS occurs around $\theta \approx \pi / 4$ and $5\pi / 4$, Δu_{N} becomes negative at these locations. This shows that the locations around $\theta \approx \pi / 4$ and $5\pi / 4$ are infeasible sites from a view-point of the misfit of plastic deformation. A large amount of GBS is needed for the formation of grain-boundary cracks. However, in addition to the occurrence of GBS, the misfit of plastic deformation at grain boundary affects the formation of grain-boundary cracks. Figures 8(a) and (b) show the feasible and infeasible sites for the formation of the grain-boundary cracks shown in Figs. 5(a) to (d).

5. Summary

Using a double cylindrical bicrystal of a Cu-SiO_2 alloy, tensile tests were performed at 800K under $2\times10^{-4}/\mathrm{s}$. Three specimens cut from the same double cylindrical bicrystal were deformed to three different strains. Grain-boundary cracks were observed at diagonal locations on a circular grain boundary where a large amount of GBS occurred. However, although a similar large amount of GBS occurred at the other diagonal locations, no cracks were observed there. These feasible and infeasible sites for the formation of grain-boundary cracks are explained by considering plastic deformation of the IS and OS grains. In addition to the occurrence of GBS, the misfit of plastic deformation at the grain boundary affects the formation of grain-boundary cracks in the double cylindrical bicrystal. The effect of the misfit of plastic deformation is important in polycrystals where most of the grains are embedded in and surrounded by other grains.

Acknowledgements

The present work was supported by the by a Grant-in-Aid for Scientific Research from the Ministry of Education, Culture, Sports, Science and Technology of Japan. The authors would like to thank Dr. Kuniteru Mihara in Furukawa Electric Co.,Ltd. for suppling an alloy ingot.

REFERENCES

1) S. Onaka, S. Soeta, M. Kato and R. Tanaka: J. Mat. Sci. **23**(1988), 577-582.

2) H. Andoh, J. Sugita, S. Onaka and S. Miura: J. Mat. Sci. Lett. **9**(1990), 314-315.

3) S. Onaka, F. Tajima, S. Hashimoto and S. Miura: Acta Met. Mat. **43**(1995), 307-311.

4) H. Miura, T. Sakai, T. Otsuka, R. Monzen and S. Onaka: Acta Mat. **48**(2000), 1959-1966.

5) A. Otsuki and M. Mizuno: Proc. Symp. On Grain Boundary Structure and Related Phenomena, Trans. Japan Inst. Metals, Suppl. **27**(1986), 789-796.

6) A. Otsuki: Mat. Sci. Forum **207**-**209**(1996), 413-416.

7) H. Miura, T. Sakai and G. Gottsein: J. Mater. Res. **13**(1998), 3100-3105.

8) H. Sato, T. Fujii, S. Onaka and M. Kato: J. Mat. Sci. **38**(2003), 1689-1693.

9) Y. Matsubara, H. Saito, H. Okada, T. Fujii, S. Onaka and M. Kato: J. Japan Inst. Metals **67**(2003), 398-403.

Figure captions

Fig. 1 The double cylindrical bicrystal of Cu-0.032mass%Si consisting of IS and OS grains used in the present study. (a) Illustration of the shapes of a bicrystal and a grain boundary in the bicrystal and (b) optical micrograph showing a round slice cut from the bicrystal.

Fig. 2 The tensile specimen cut from the double cylindrical bicrystal. (a) The shape and (b) a pair of stereographic projections showing the orientations of the grains IS and OS. The angle θ measured from the stress axis (the x_1-axis) shown in Fig. 2(a) is used to indicate locations on the circular grain boundary. The marks in Fig. 2(b) show the slip systems expected to operate in each grain.

Fig. 3 The nominal stress-plastic strain curves of the double cylindrical bicrystal of the Cu-SiO_2 alloy at 800K under 2×10^{-4} / s . Deformation of specimens D1, D2 and D3 cut from the same bicrystal was interrupted at $\varepsilon\approx0.02$, 0.04 and 0.18, respectively.

Fig. 4 Variation in the amount d of grain-boundary sliding as a function of the angle θ defined in Fig. 2(a) for specimen D1 which was deformed until $\varepsilon\approx0.02$.

Fig. 5 Optical micrographs showing the surface of specimen D2 which was deformed until $\varepsilon\approx0.04$. Although grain-boundary cracks are observed in Figs. 5(a) and (d), no cracks are observed in Figs. 5(b) and (c).

Fig. 6 Optical micrographs showing a large grain-boundary crack in specimen D3 which was deformed until $\varepsilon\approx0.18$.

Fig. 7　Shape change of the (a) IS and (b) OS grains when uniform plastic deformation caused by the slip systems shown in Fig. 2(b) takes place.

Fig. 8　Variation in the normal component Δu_{N} of the difference in the displacements $\Delta \boldsymbol{u} = \boldsymbol{u}^{\mathrm{O}} - \boldsymbol{u}^{\mathrm{I}}$ along a circular grain boundary in the double cylindrical bicrystal. (a) Illustration of variation in Δu_{N} and (b) normalized variation $\Delta u_{\mathrm{N}} / (\gamma r)$ as a function of θ, where r is the radius of the circular grain boundary.

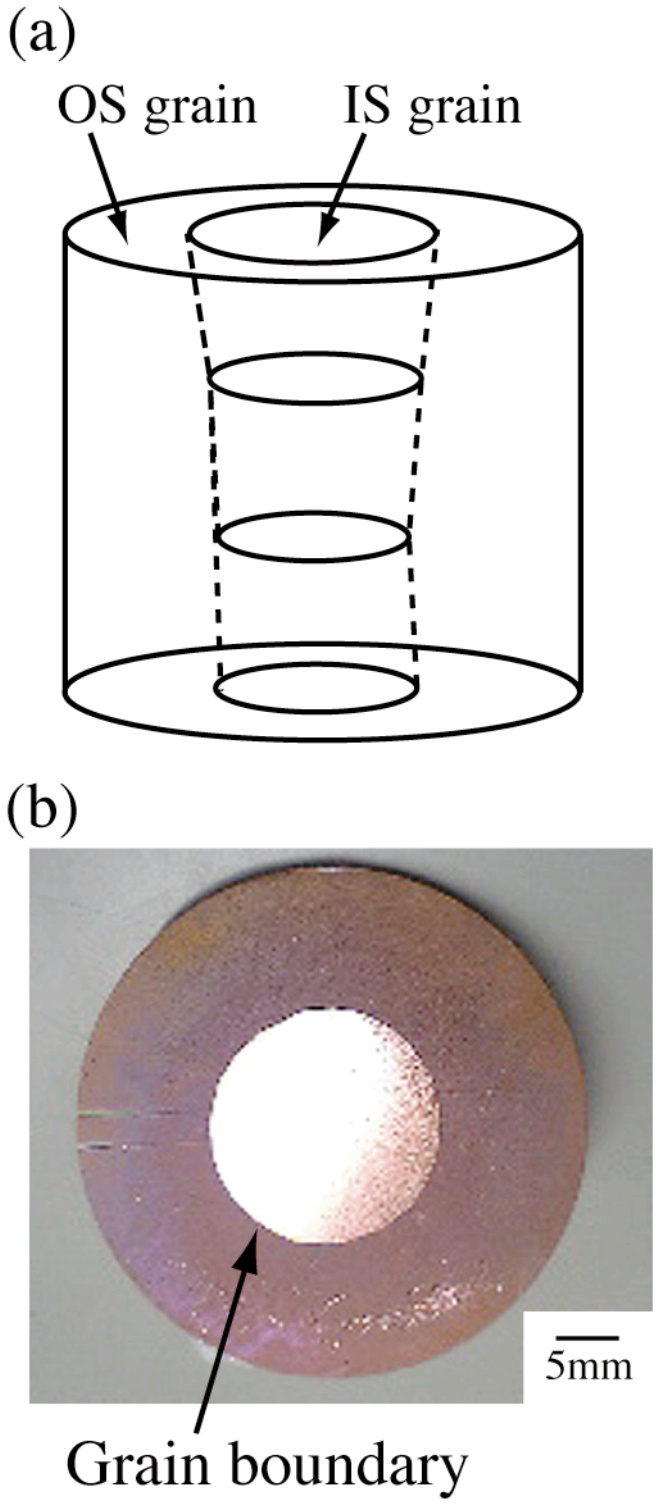

Fig. 1

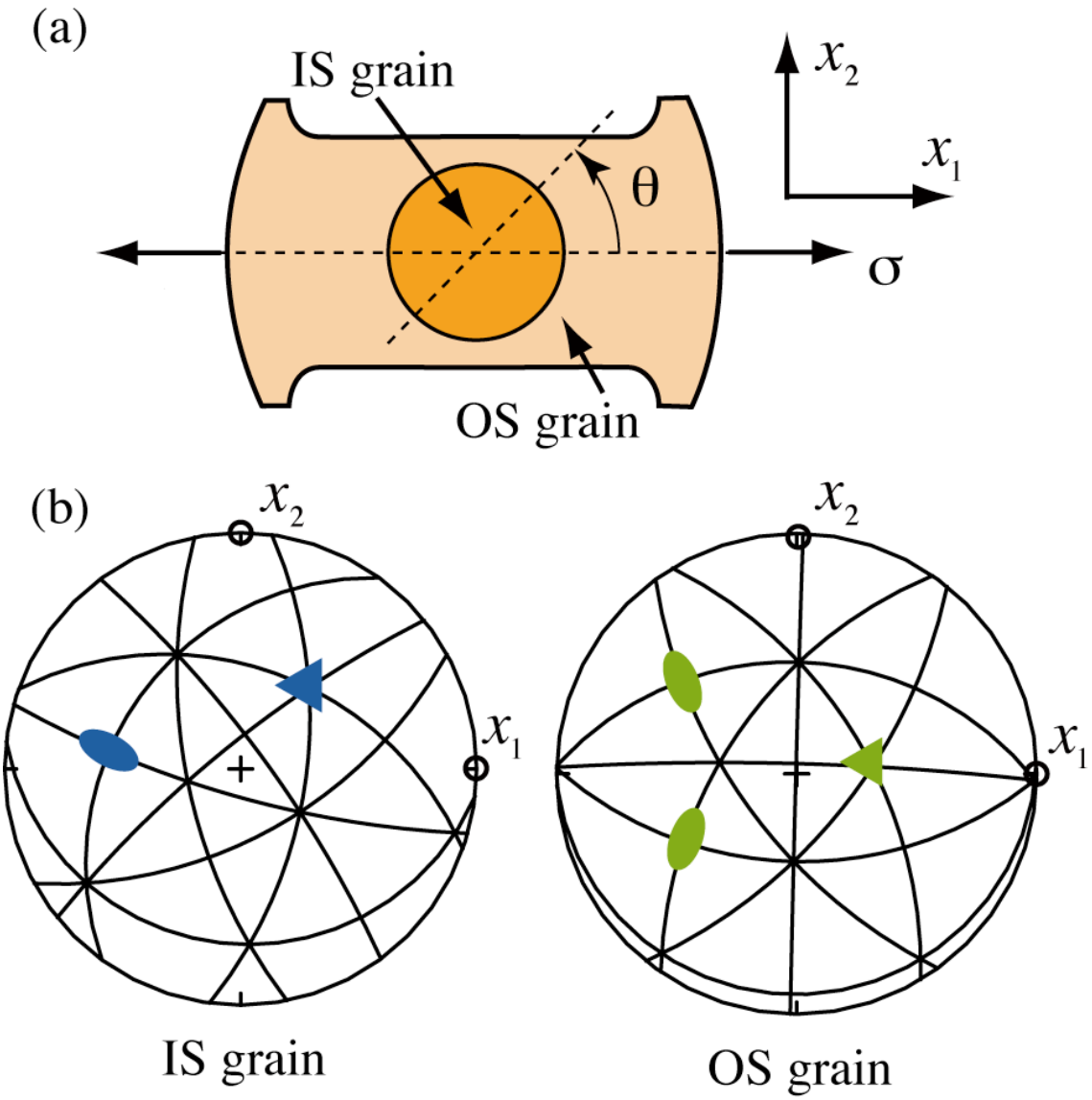

Fig. 2

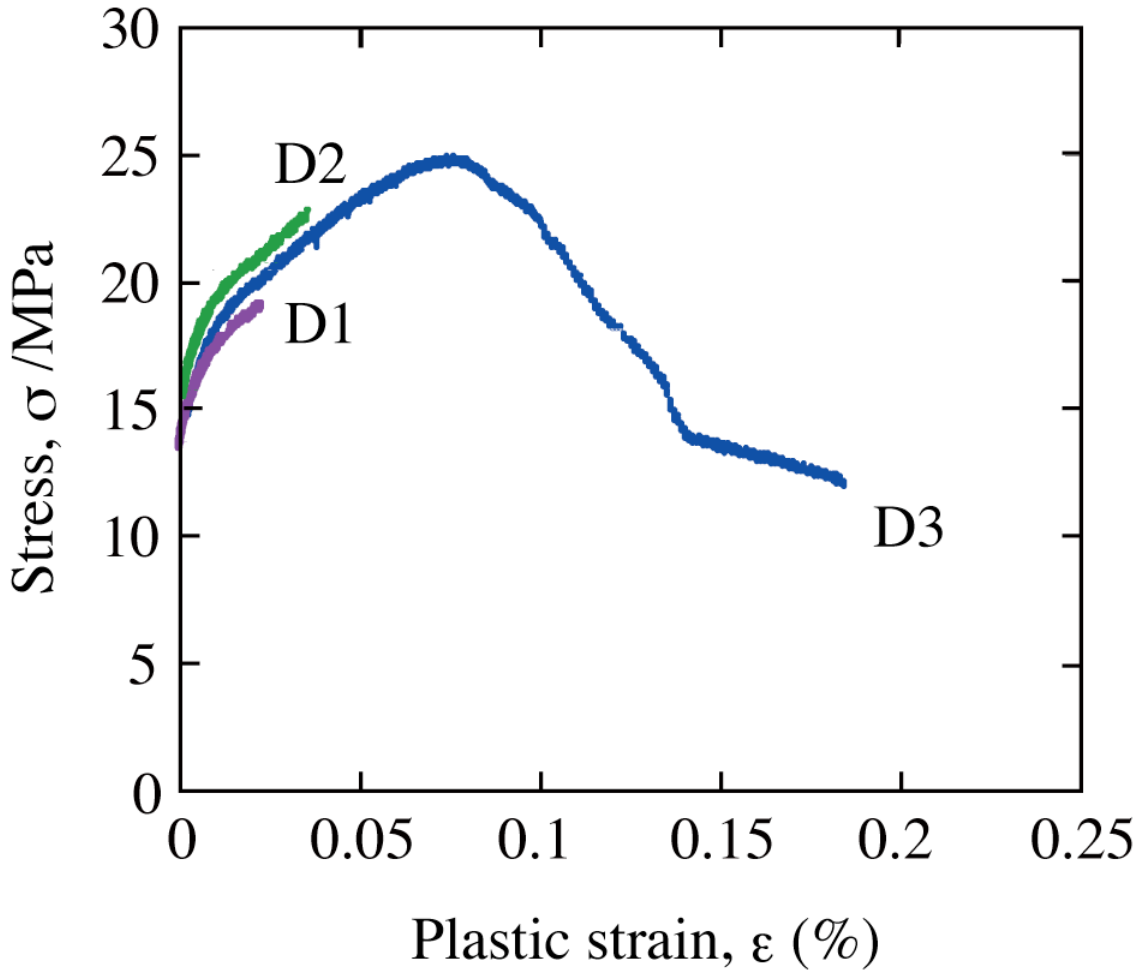
30
25
20
15
10
5
0
0
0.05
0.1
0.15
0.2
0.25
D2
D1
D3
Stress, σ /MPa
Plastic strain, ε (%)

Fig. 3

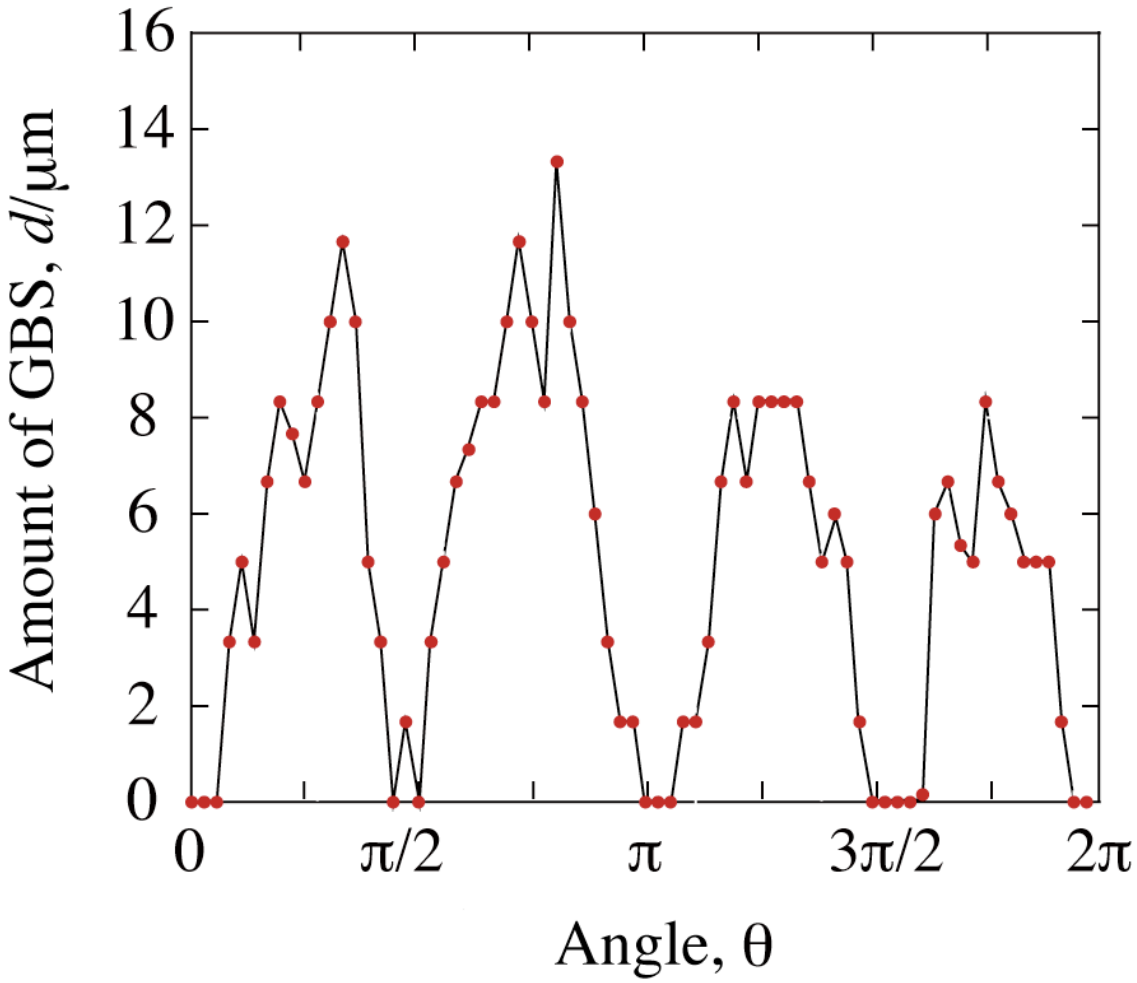

Fig. 4

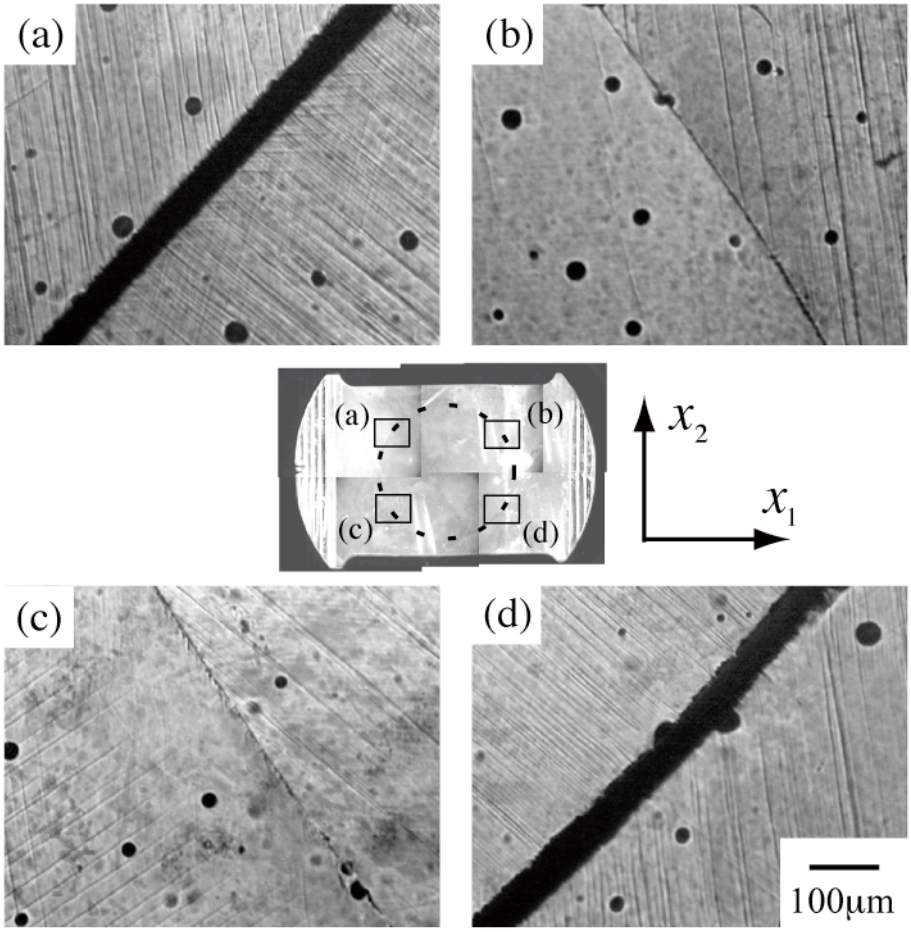

Fig. 5

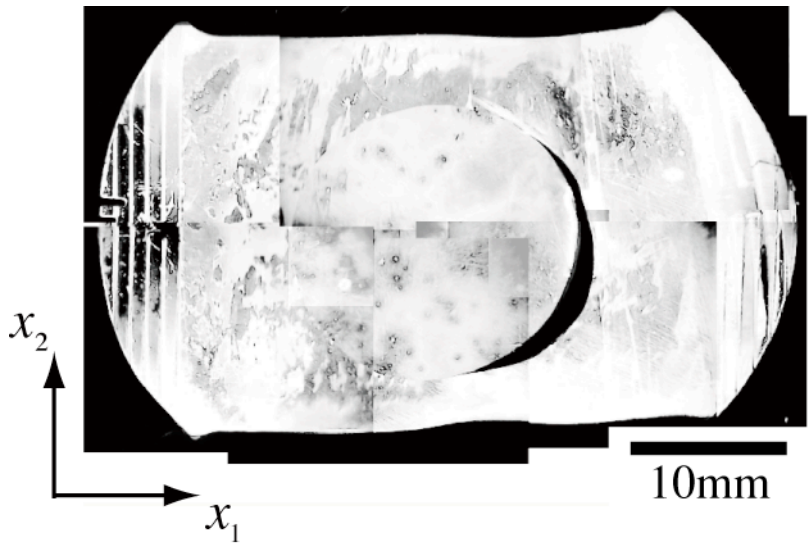

Fig. 6

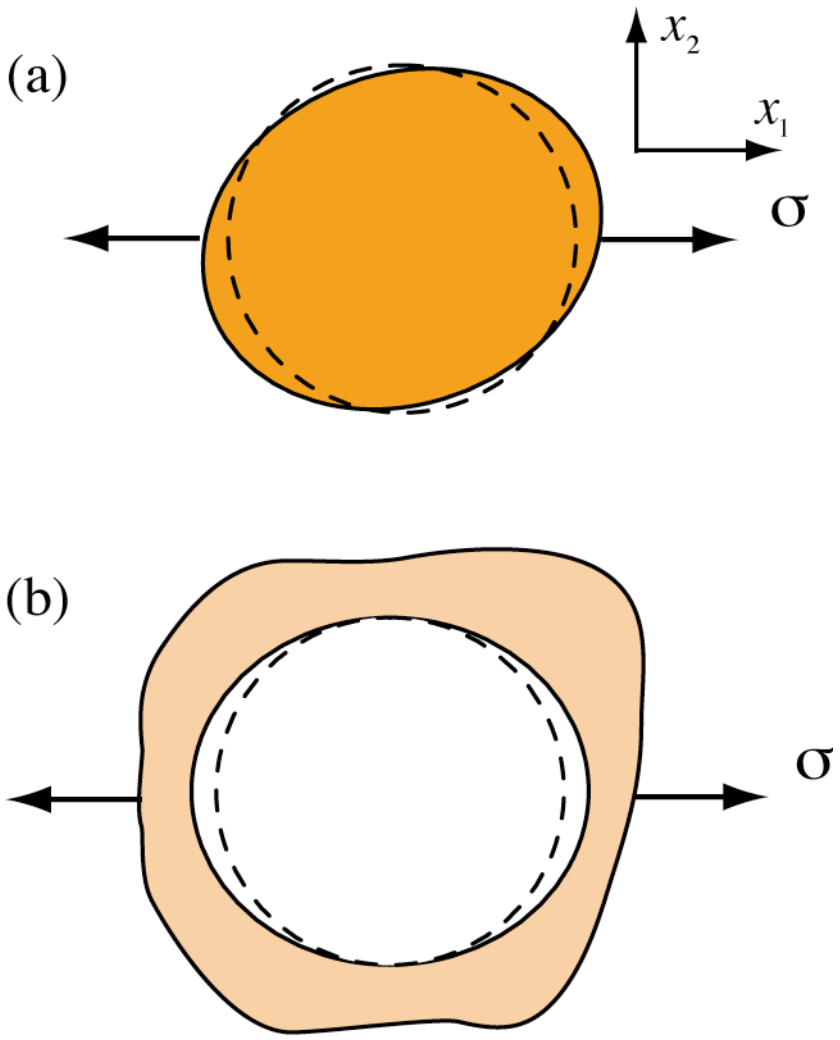

Fig. 7

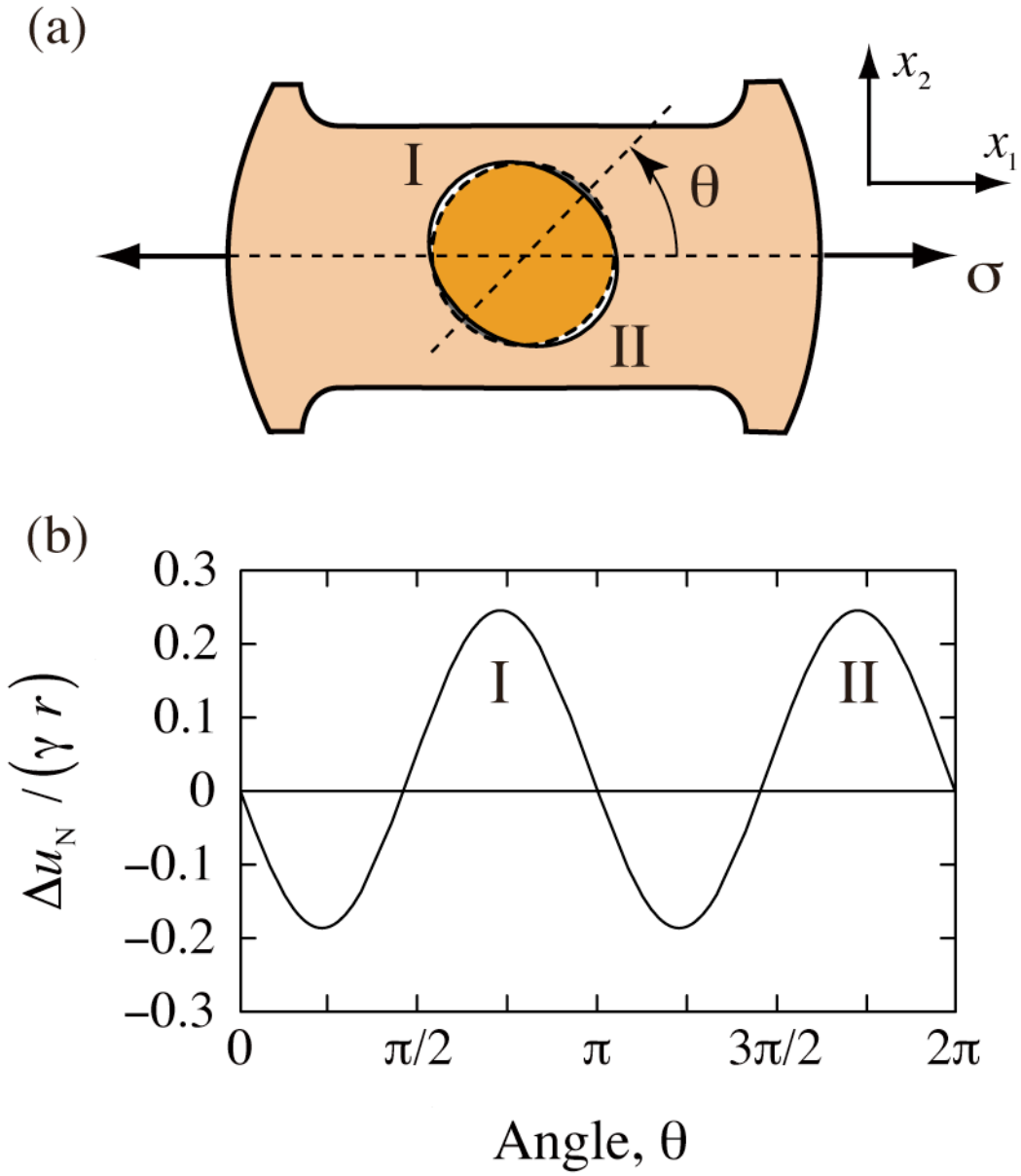
(a)
x_2
x_1
I
θ
σ
II
(b)
0.3
0.2
0.1
0
–0.1
–0.2
–0.3
$\Delta u_N / (\gamma r)$
I
II
0
π/2
π
3π/2
2π
Angle, θ

Fig. 8